applied sciences

MDPI

Article

Partial Discharge Type Identification of 10 kV T-Type Terminal Based on Empirical Mode Decomposition and Deep Convolution Neural Network

Shude Cai *, Chunhua Fang, Yongyu Guo, Jialiang Liu and Gu Zhou

School of Electrical and New Energy, Three Gorges University, Yichang 443002, China; fang107531@163.com (C.F.); 202208580121065@ctgu.edu.cn (Y.G.); 202208080021031@ctgu.edu.cn (J.L.); 202208080021059@ctgu.edu.cn (G.Z.)
* Correspondence: 202208580121006@ctgu.edu.cn; Tel.: +86-15990782572

Featured Application: In this paper, the partial discharge characteristic waveform is decomposed by EMD to obtain more characteristic signals for DCNN training and recognition.

Abstract: As a relatively weak part of cable insulation, T-type cable terminals will have insulation defects due to process, installation, and other problems, resulting in partial discharge. Therefore, this paper uses Deep Convolution Neural Network (DCNN) and Empirical Mode Decomposition (EMD) to identify the partial discharge type of a 10 kV T-type cable terminal. This method uses the partial discharge experimental platform of the T-type cable terminal to collect the partial discharge signal. After the original signal that is difficult to identify is decomposed by EMD, a series of intrinsic mode components (IMFs) that are easy to locate are obtained. The deep learning network model is used to identify the defect type of the IMF signal. The results show that the overall defect recognition rate of this method reaches 95.3%. Compared with the traditional random forest algorithm (RF), the 10 kV T-type terminal partial discharge type recognition method based on EMD–DCNN is considered in this paper. The recognition accuracy of the main insulation scratch, bushing fouling, and joint loosening defects is higher than that of the traditional mechanical learning algorithm, RF, indicating that the method adopted in this paper can more effectively and accurately identify the defect type.

Keywords: partial discharge; T-type cable terminal; defect type; deep learning; empirical mode decomposition

Academic Editors: Andreas Sumper and Gerard Ghibaudo

Received: 8 February 2025
Revised: 25 March 2025
Accepted: 2 April 2025
Published: 3 April 2025

Citation: Cai, S.; Fang, C.; Guo, Y.; Liu, J.; Zhou, G. Partial Discharge Type Identification of 10 kV T-Type Terminal Based on Empirical Mode Decomposition and Deep Convolution Neural Network. *Appl. Sci.* **2025**, *15*, 3962. https://doi.org/10.3390/app15073962

1. Introduction

The T-type cable terminal can improve the space utilization rate and safety of the 10 kV distribution network. As a relatively weak part of the cable insulation, the cable terminals will have insulation defects due to problems such as process and installation, causing partial discharge (PD). Once the T-type cable terminal has a partial discharge, it will cause serious harm to the stability of the distribution network. Therefore, accurately identifying the partial discharge type of the T-type terminal is conducive to evaluating the harmfulness of partial discharge defects and formulating corresponding solutions [1–6]. However, the original partial discharge signal obtained by experiments has a large amount of redundant and useless information, and there are problems such as similarity and difficulty in identifying each defect feature, which greatly affect the accuracy of signal feature recognition. In

addition, there are some problems such as overfitting in partial discharge identification [7,8]; overfitting will affect the speed and accuracy of defect feature recognition.

For PD signal feature recognition, domestic and foreign scholars have performed a lot of work. Zhang used a digital notch filter to suppress periodic interference. Although this method has a certain filtering effect on interference, its ability to suppress interference is limited, resulting in a poor recognition effect [9]. Ramy Hussein and other scholars have studied the feature extraction method of using a fast Fourier transform to obtain the spectrum of the partial discharge signal when there is noise interference and the partial discharge feature with a low-frequency component as input. However, the recognition effect is poor due to the general effect of the obtained feature spectrum [10]. Aiming at the frequent defects in the field, Ab Halim designed five kinds of XLPE cable joints and also proposed a feature extraction method based on high anti-noise principal component analysis (PCA). Compared with traditional input features such as statistics and fractals, artificial neural networks (ANNs) and support vector machines (SVMs) were used for classification. However, PCA is a linear dimension reduction method, assuming that there is a linear relationship between data features, while the actual partial discharge signal may contain nonlinear features, resulting in the loss of key nonlinear information [11]. Huang Xuexiao used partial discharge pattern recognition of switchgear; but the application scope of this method is limited, the recognition accuracy is low, and its performance depends on the deep network structure. When the number of network layers increases, the performance will decrease, resulting in a series of problems such as information loss [12], resulting in low recognition accuracy. Mao Zhenyu used the BPNN (Back Propagation Neural Network) to identify the partial discharge type of insulation defects of T-type cables. However, because the feature is artificial, it is a subjective method. It is impossible to fully express the essential characteristics of the signal. Although the influence can be reduced by the selection of a certain feature object, its huge workload greatly reduces the efficiency [13]. C. Mazzetti proposed a partial discharge identification method for cable terminals based on an adaptive fuzzy logic network. By setting different fuzzy rule parameters, the partial discharge caused by different defects of the cable terminal is identified. However, due to the subjectivity and complexity of fuzzy rule parameter setting, the recognition accuracy is affected [14]. The advantages and disadvantages of the above research are shown in Table 1.

Table 1. Advantages and disadvantages of current research on partial discharge characteristics.

Researcher	Method	Merit	Defect	Contribution
Zhang [9]	A digital notch filter is used to suppress periodic interference.	Certain filtering effect.	The ability to suppress interference is limited, resulting in poor performance.	Through the organic combination of experimental modeling and spectrum analysis, Zhang solved the problem that it is difficult to accurately identify the fault type in PD detection and promoted the leap from qualitative judgment to quantitative analysis of insulation diagnosis of high-voltage equipment.
Ramy Hussein [10]	The spectrum of partial discharge signal is obtained by the fast Fourier transform.	More effective extraction of partial discharge spectrum from interference.	There is still some interference in the partial discharge spectrum.	The research of Hussein solved the problem of feature degradation and misclassification of acoustic partial discharge detection in a strong noise environment through noise robustness enhancement, feature engineering innovation, and a hybrid intelligent classification framework design.

Table 1. *Cont.*

Researcher	Method	Merit	Defect	Contribution
Ab Halim [11]	Feature extraction method based on high anti-noise principal component analysis (PCA).	Good denoising effect.	PCA is a linear dimension reduction method, which cannot deal with nonlinear signals.	Through the collaborative design of noise modeling, multi-modal robust feature extraction, and transfer learning classification framework, Raymond overcame the problem of feature degradation and misclassification of XLPE cable joint partial discharge detection in a high noise environment.
Huang [12]	Partial discharge pattern recognition of the switch cabinet is adopted.	It can effectively identify the early discharge signal of insulation defects.	The scope of application is limited.	By improving the ResNet architecture, optimizing the time–frequency representation and noise robustness design, Huang significantly improved the recognition accuracy and engineering applicability of the partial discharge mode of the switchgear.
Mao [13]	BP is used for PD feature recognition.	The nonlinear characteristics of partial discharge signals can be captured by a multi-layer structure.	The huge workload greatly reduces the efficiency.	Through algorithm improvement and systematic verification, Mao established the effectiveness of the BP neural network in cable partial discharge identification and provided a new tool for smart grid fault diagnosis.
C. Mazzetti [14]	A partial discharge identification method of cable terminal based on an adaptive fuzzy logic network.	It is suitable for dealing with complex scenes with on-site noise interference or signal overlap.	Due to the subjectivity and complexity of fuzzy rule parameter setting, the recognition accuracy is affected.	C. Mazzetti solved the problem of noise sensitivity and interpretability in PD pattern recognition of cable accessories through the innovative application of neural fuzzy network, which has both a theoretical breakthrough and engineering practical value.

The empirical mode decomposition (EMD) can obtain the intrinsic mode function, and the useless information is filtered out. The filtering effect is higher than the other filtering methods, and only the IMF containing the characteristic signal is left. The IMF signal as the input of the classifier will greatly improve the recognition accuracy [15]. Deep convolutional neural networks (DCNNs) are widely used in various fields [16–19]. It can effectively alleviate the phenomenon of gradient disappearance and overfitting. It has the advantages of short training time and stable convergence, which can effectively improve recognition accuracy [20,21]. Therefore, this paper proposes a method based on empirical mode decomposition and deep convolutional neural network (DCNN) for partial discharge type identification of a 10 kV T-type terminal. In this method, the partial discharge signal obtained by the experiment is decomposed by EMD, and the IMF signal is obtained and used as the input of the deep convolutional neural network. Compared with the EMD-SVD-RF method, the effectiveness of the proposed method is verified.

2. The Basic Theory of EMD and DCNN

2.1. The Basic Theory of Empirical Mode Decomposition

EMD uses time scale characteristics to decompose, which makes EMD have a good effect on the processing of nonlinear signals. EMD can retain the advantages of time-frequency localization in wavelet transform and overcome the difficulty of selecting a wavelet basis function in wavelet transform because it does not need a basis function. In

this paper, this method is used to process the partial discharge signal of the T-type terminal, and a series of signals containing characteristic components are obtained.

EMD can decompose the original signal into multiple intrinsic mode functions containing characteristic components (IMFs) [22–24]. Among them, the IMF has two characteristics: (1) the number of zero-crossing points and the number of extreme points differ by at most one; (2) at any time, the average value of the extreme envelope is 0. The EMD process for any signal $x(t)$ is as follows:

By fitting all the extreme points of the initial signal $x(t)$ with its corresponding envelopes $e_+(t)$ and $e_-(t)$, let the average values of $e_+(t)$ and $e_-(t)$ be the mean envelope $m_1(t)$ of $x(t)$. The corresponding expression is as follows:

$$m_1(t) = \frac{e_+(t) + e_-(t)}{2} \tag{1}$$

Among them, $m_1(t)$ is the mean envelope of the initial signal $x(t)$, $e_+(t)$ and $e_-(t)$ are all extreme points of the initial signal $x(t)$ and their corresponding envelopes.

Using $x(t)$ minus $m_1(t)$ as the signal $h_1^1(t)$ to remove the low-frequency signal:

$$h^1{}_1(t) = x(t) - m_1(t) \tag{2}$$

In general, $h_1^1(t)$ is a non-stationary signal, so $h_1^1(t)$ does not meet the characteristic conditions of IMFs. By continuously carrying out the above steps, until the nth time, the signal $h_1^n(t)$ satisfying the above conditions is obtained, and the first-order IMF component is as follows:

$$c_1(t) = imf_1(t) = h^n{}_1(t) \tag{3}$$

Among them, $imf_1(t)$ is the first-order IMF component, and $c_1(t)$ is equal to the first-order IMF component $imf_1(t)$.

By subtracting $c_1(t)$ from the initial signal, a new signal $r_1(t)$ is obtained, which eliminates the high-frequency part:

$$r_1(t) = x(t) - c_1(t) \tag{4}$$

The second-order IMF component $c_2(t)$ is obtained by obtaining $c_1(t)$ for $r_1(t)$, and the above steps are repeated many times until the nth-order IMF component $c_n(t)$ or the residual $r_n(t)$ is less than the set value, which indicates that the EMD signal separation is completed, and $x(t)$ is decomposed into:

$$x(t) = \sum_{i=1}^{n} c_i(t) + r_n(t) \tag{5}$$

Among them, $r_n(t)$ is the residual, representing the general trend of the signal, $x(t)$ is the initial signal, and $c_i(t)$ is the ith-order IMF component.

2.2. Deep Convolutional Neural Network

The structure of DCNN is shown in Figure 1 [25–28]. The convolution layer is the most important part of DCNN. There are multiple feature maps on the convolution layer, and each feature map is connected to the feature map of the previous layer through the convolution kernel. The convolution kernel acts on the feature map, sets the corresponding step size, and moves through the step size to obtain the characteristics of the input signal. Each activation layer is located after the convolution layer, and the linearly inseparable part is removed to achieve the purpose of linear separability.

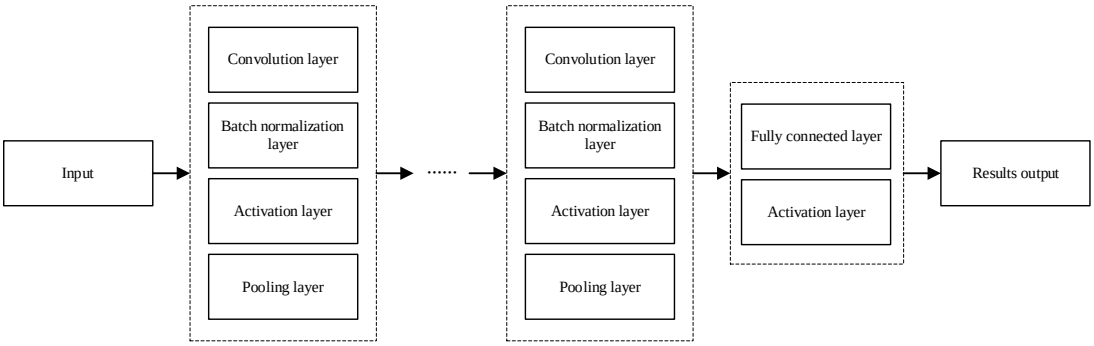

Figure 1. Structure diagram of DCNN.

The role of the pooling layer is to replace the output of the signal in the segment according to the overall trend of the adjacent part. The advantage of this is that the parameters and dimensions of the output of the segment can be reduced, thereby accelerating the operation speed and greatly reducing the occurrence of overfitting.

The role of the batch normalization layer is to solve the distribution changes in the intermediate layer data. It can also speed up the convergence speed and is more stable and faster when training models with more layers.

The function of the fully connected layer is to combine the above features and connect all the nodes of the upper layer to achieve the purpose of classifying the features.

3. T-Head Cable Partial Discharge Signal Acquisition

3.1. Experimental Principle and Platform

The schematic diagram of the partial discharge experiment principle of the T-type terminal is shown in Figure 2. When the T-terminal produces partial discharge, the current signal flows into the ground wire. The current signal is collected by HFCT and stored in the digital oscilloscope. The digital oscilloscope is connected to the PC, and the collected partial discharge signal is analyzed by the PC.

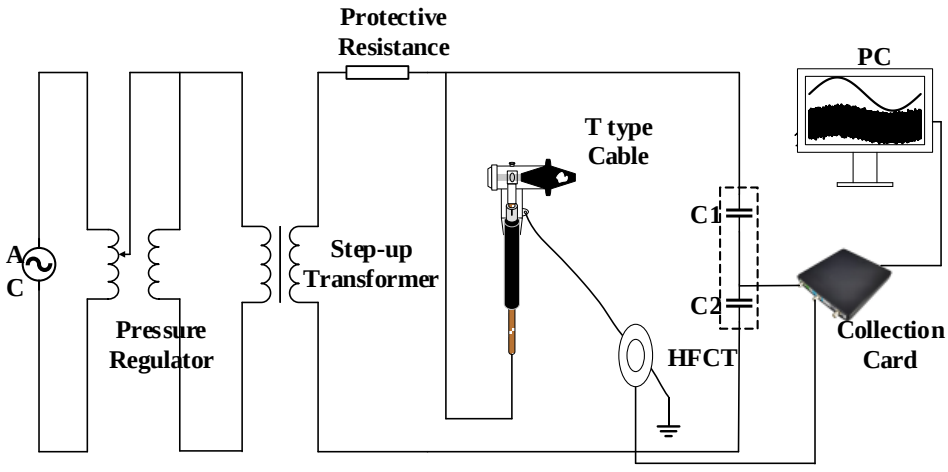

Figure 2. Schematic diagram of T-type terminal office discharge experiment.

To reduce interference, the experiment was carried out in an electromagnetic shielding room. The noise of the shielding room is about 1 pC. The equipment required for the experiment is as follows: a digital oscilloscope, 220 V AC power supply, test console, HFCT, capacitive voltage divider, transformer, etc. The transformer selects the transformer without partial discharge, and its rated capacity is 150 kVA. The rated voltage of C1 and C2 voltage dividers is 200 kV, the high-voltage parameters are R = 800 MΩ and C = 75 pF,

the low-voltage parameters are R = 0.08 MΩ and C = 750 nF, and the voltage ratio is 10,000:1. HFCT uses a broadband (100 kHz–50 MHz) self-integrating Rogowski coil for partial discharge measurement [29]. The highest sampling rate of the digital oscilloscope used can reach 600 MHz, and the sampling rate of this experiment is 100 MHz. Some equipment parameters are shown in Table 2. The composition of the acquisition system and the experimental wiring diagram of the partial discharge platform are shown in Figures 3 and 4.

Table 2. Some equipment parameters.

Equipment	Rated Capacity	High-Pressure Parameters	Low-Pressure Parameters	Load Division Ratio
Voltage divider	200 kVA	R = 800 MΩ, C = 75 pF	R = 0.08 MΩ, C = 750 nF	10,000:1

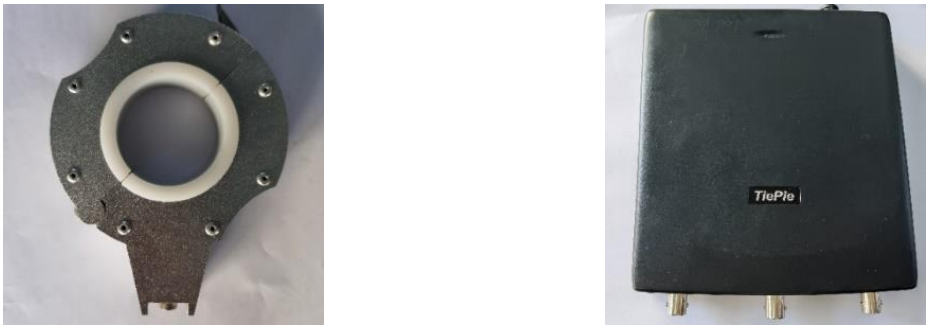

(**a**) high-frequency current sensor (**b**) digital oscilloscope

Figure 3. Acquisition system.

Figure 4. Experimental platform.

3.2. Defect Types of T-Joints

Through a literature review, this paper designs three common defect models of partial discharge of T-joints. The defect models are as follows: (1) damage caused by workers construction and installation, or a series of improper operations. Such damage will not cause problems in the short term but will cause partial discharge under long-term operation. The length, width, and depth of the scratch on the insulation surface are set to 40 mm, 2 mm, and 2 mm, respectively; 30 mm, 2 mm, 2 mm; 20 mm, 2 mm, 2 mm; and other groups

of data. As shown in Figure 5a, (2) due to improper installation or long-term operation, the surface has not been cleaned, resulting in stains on the nozzle sleeve and causing partial discharge. The solution of sodium chloride, silicon dioxide, and water in a ratio of 1:2:2 is mixed to simulate the stain of the casing. The surface of the casing is treated with 3 drops, 6 drops, and 9 drops of solution to simulate the partial discharge phenomenon, as shown in Figure 5b. (3) Due to the improper installation of the T-joint during the construction of the workers, the joint looseness between the pair of nozzle sleeves occurs due to failure to tighten and other reasons, resulting in partial discharge. In this experiment, this type of partial discharge defect uses a knob to the middle position of the joint, a knob to a quarter position of the joint, and a knob to a quarter position of the joint to simulate joint loosening, as shown in Figure 5c.

(**a**) Main insulation scratch (**b**) Casing fouling (**c**) Loose joint connection

Figure 5. Defect model diagram.

3.3. Experimental Acquisition Method of Partial Discharge Signal

The pressurization methods of the partial discharge test include the constant pressure method and the step-by-step pressurization method. The constant voltage method is to apply a constant initial discharge voltage to the insulation in the sample until the insulation is broken down. Although this method is most in line with the actual insulation working voltage situation, it takes a long time. The step-by-step voltage method can quickly realize the whole process of simulated discharge, obtain a large number of experimental data, and greatly improve the experimental speed. The constant pressure method and the constant voltage method have the same insulation aging effect. Therefore, the step-by-step voltage method with faster speed is adopted in this paper.

The data samples under different defects were collected in the experiment with 0.02 s as the cycle. According to the experimental platform shown in Figure 4, the voltage is quickly raised to the rated voltage of the joint U_0 = 8.7 kV. If there is a discharge phenomenon, the voltage applied at this time is recorded, and if there is no discharge phenomenon, the voltage is continuously raised. Under the same conditions as the above conditions, the five data samples were measured, and the mean value of the five data samples was taken as the initial discharge voltage. The initial discharge data of different defects are obtained by working for 0.5 h at the initial discharge voltage. The initial discharge voltage of the defects obtained by the experiment is shown in Table 3. According to the table, the initial discharge voltage of the insulation scratch defect is close to the rated voltage of the joint of 8.7 kV, while the other two defects are greater than the rated voltage of the joint of 8.7 kV.

To accelerate the deterioration of insulation, a staged step-up method is adopted. Starting from the initial discharge voltage, each voltage gradient is about 5 kV, each voltage gradient is maintained for 30 min, and data samples are collected until the discharge becomes serious (such as the number of discharge pulses becomes dense and the experimental site hears a significant discharge current sound). The pressurization is

stopped, data are collected, the above steps are repeated for each defect, and each defect is repeated ten times.

Table 3. Initial discharge incipient discharge voltage.

Defect Type	Insulation Scratch (40 mm, 2 mm, 2 mm)	Casing Fouling	Joint Looseness (1/2 Place)
Voltage/kV	8.7	10.7	11.7
	9	10.9	12.1
	9.1	10.8	12.1
	9	11	12.4
	8.1	10.7	12.2
Mean value/kV	8.8	10.8	12.1

Affected by the experimental environment, the collected current signal will be affected by noise and low-amplitude stray pulses. These irrelevant signals need to be filtered. The EMD filtering method is a commonly used signal noise filtering method. In this paper, EMD filtering is used to filter out the noise signal, and the specific process is not described too much.

After EMD filtering, the partial discharge test waveforms of the three defects are shown in Figures 6–8, respectively.

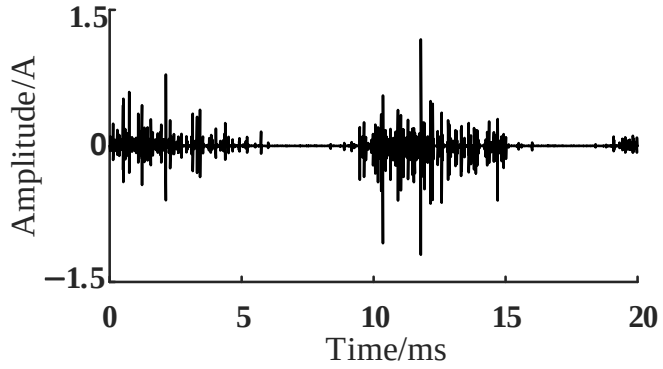

Figure 6. Waveform diagram of an insulation scratch defect.

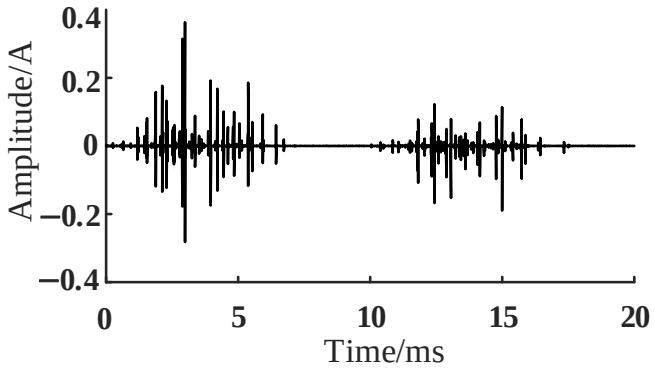

Figure 7. Waveform diagram of fouling defect.

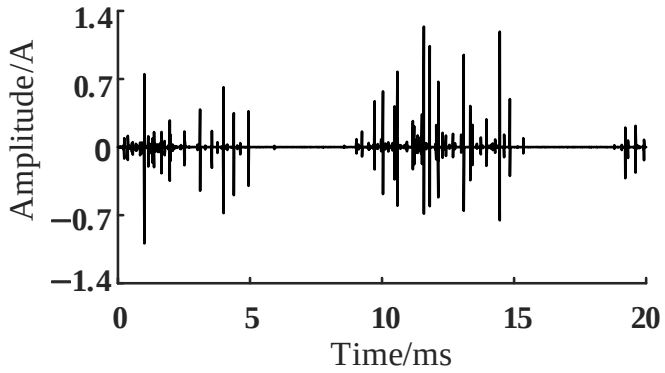

Figure 8. Waveform of joint loosening defect.

The distribution of partial discharge amplitude–pulse width–discharge times of each defect is shown in Figures 9–11. The discharge times of different defects are different. The distribution range of partial discharge amplitude and pulse width of insulation scratch is mainly concentrated in the range of [−1,1] A and [0.08,0.12] μs, and the maximum amplitude and maximum pulse width are 1.75 A and 0.47 μs, respectively. The length of the discharge amplitude distribution interval of the casing fouling is narrow, but the discharge distribution is more uniform, and the approximate "pyramid" type concentrated area can be observed. The pulse width amplitude of the loose joint is distributed in a "one-character" shape along the x-axis, and the maximum amplitude and the length of the amplitude distribution interval are larger than the other two types of defects.

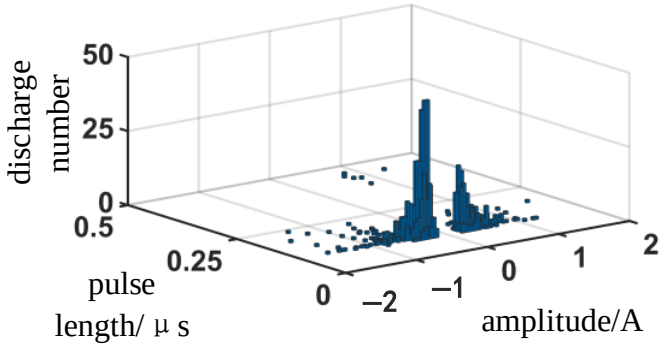

Figure 9. Insulation scratch defect amplitude–pulse width–discharge times diagram.

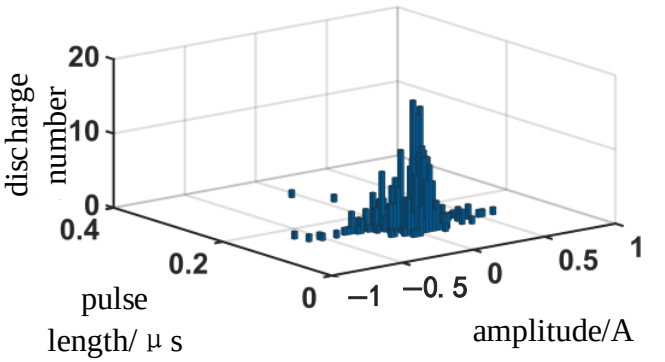

Figure 10. Casing fouling defect amplitude–pulse width–discharge times diagram.

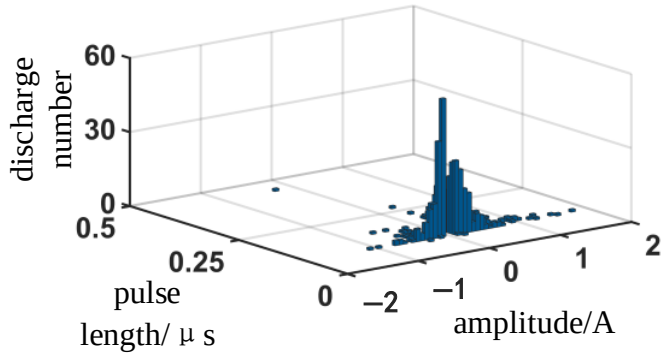

Figure 11. Joint looseness defect amplitude–pulse width–discharge times diagram.

4. EMD and DCNN Partial Discharge Type Recognition

4.1. EMD and DCNN Partial Discharge Type Identification Process

The flow chart of EMD and DCNN partial discharge type recognition is shown in Figure 12.

(1) The original partial discharge signal x (t) of the three defects is obtained by collecting the partial discharge signal of the T-head cable. The original partial discharge signal x (t) is decomposed by EMD after noise reduction, and the intrinsic mode IMFi (t) component of the original partial discharge signal x (t) of the three defects is obtained.

(2) The intrinsic mode IMFi (t) component separates the training samples and the test samples at a ratio of 8:2, and the DCNN network trains the training samples. Through the training of sample training, the T-type terminal partial discharge type recognition classifier is obtained.

(3) The test sample set is used to test the T-type terminal partial discharge type recognition classifier, test the validity and correctness of the model, and adjust the parameters. The final model is applied to the identification of the T-type terminal partial discharge type, and the corresponding recognition results are obtained.

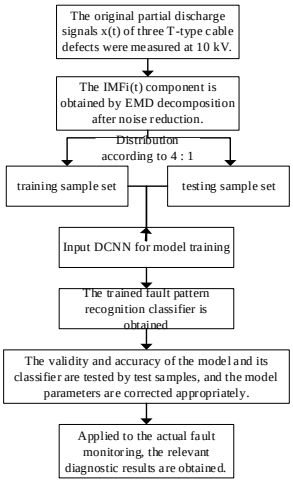

Figure 12. Flowchart of EMD–DCNN release type identification.

4.2. EMD and DCNN Partial Discharge Type Identification Analysis

Partial discharge signal is a key feature to reflect the insulation state of power equipment, but it usually has the characteristics of non-linearity, non-stationarity, and strong noise interference. Traditional methods (such as the Fourier transform and wavelet analysis) have limitations in dealing with such signals. As an adaptive signal decomposition method,

empirical mode decomposition has the following two main advantages in dealing with partial discharge signals.

First, traditional signal analysis methods (such as wavelet transform) need to set the basis function in advance, which is difficult to adapt to the complex time-varying characteristics of partial discharge signals. The EMD adaptively decomposes the signal into multiple intrinsic mode functions through a "screening" process, without any prior basis function constraints. This feature enables it to accurately capture the transient pulse waveform of the partial discharge signal.

Second, partial discharge signals are often contaminated by background noise (such as white noise and periodic interference). EMD separates signal and noise through multi-scale decomposition. High-frequency IMFs (such as IMF1–IMF2) mainly contain noise components, while low-frequency IMFs (such as IMF3 and above) retain partial discharge characteristics.

The network model DCNN is built by using the MatlabR2023a Deep Learning Toolbox, the ReLU function is selected as the activation function in the network. The recognition platform is a 3.0 GHz i7 processor, and the memory is 16 GB.

To determine the parameters of the DCNN model, the partial discharge signal IMF waveform is used as input, and the identification targets are insulation scratch defect, bushing fouling defect, and joint loosening defect, respectively. This paper compares the recognition effect of the network when the learning rate is 0.01, 0.001, 0.0001, and 0.00001, respectively, as shown in Figure 13. When the learning rate is set to 0.01, although the network can quickly extract the initial features, the feature information is lost due to the fast convergence speed, and the recognition accuracy is low, indicating that the model cannot effectively capture features at high rates. By adjusting the learning rate to 0.001, the network shows progressive optimization characteristics: The recognition rate exceeds 80% when the iteration is 60 times, and the subsequent trend continues to rise. It is worth noting that when the learning rate is less than 0.001, although the model can still learn, the learning rate is significantly slower. To achieve the same recognition accuracy as the learning rate of 0.001, it takes more time to train. In addition, a learning rate that is too small can also easily cause overfitting problems. Therefore, considering the convergence speed and model stability, the learning rate of 0.001 becomes the optimal choice.

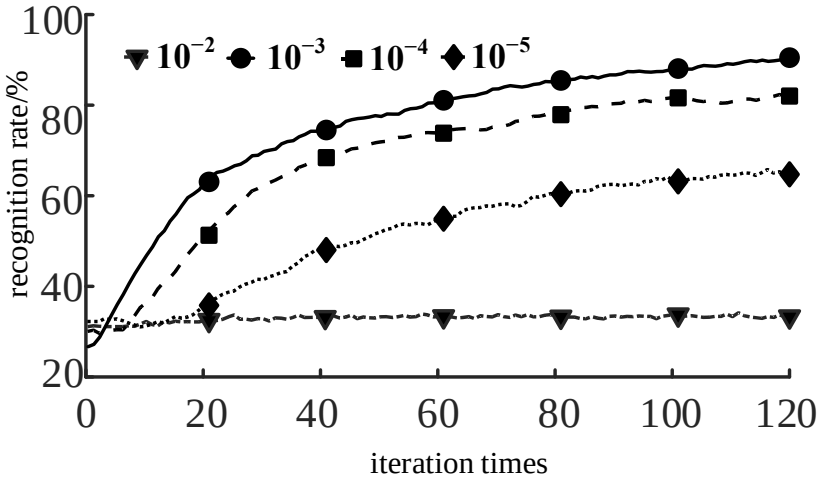

Figure 13. The recognition rate of the network under different learning rates.

The learning rate is set to 0.001, and the influence of the number of iterations on the recognition rate is analyzed. The recognition effect is shown in Figure 14. It can be seen from the recognition rate curve of the network that as the number of iterations increases, the recognition rate gradually increases and finally stabilizes at about 95%. When the

number of iterations reaches 320, the recognition rate and loss value tend to be stable. This means that the performance of the model is relatively stable at this stage. If we continue to increase the number of iterations at this time, although it may bring an extremely small performance improvement, it will consume a lot of running time, which is not cost-effective from the perspective of the input–output ratio.

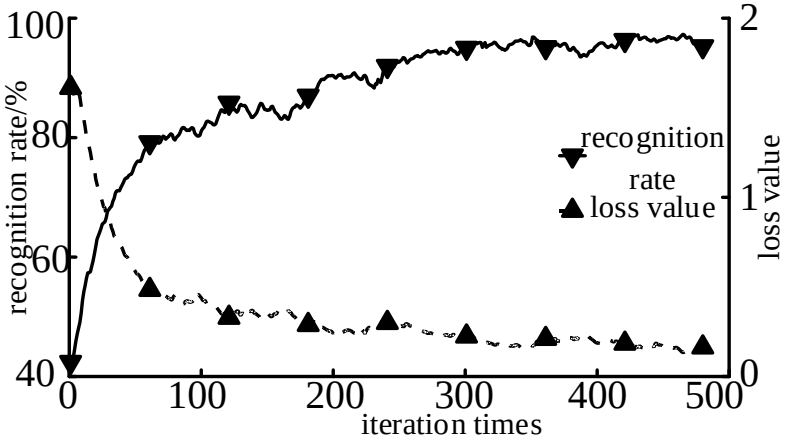

Figure 14. The influence of the number of iterations on the network.

After repeated tests, the EMD and DCNN partial discharge type recognition model is set up, and the parameters of the model are set as shown in Table 4. To ensure the accuracy of the training samples, more data are used as the input for the training samples. The partial discharge signals of the three defects are randomly classified according to the ratio of 4:1 (1200:300). Eighty percentage of the classified signals are used as the input for the training samples, and the remaining signals are the test sample set.

Table 4. DCNN parameter settings.

Network Layer	Number of Convolutional Kernels	Convolution Kernel Height × Width	Output Size	Parameter Matrix/Number of Weights	Step Size	Activation Function
Input layer			20 × 1 × 4096			
Convolution layer-1	4	9 × 1	20 × 1 × 4096	4 × 1 × 9/4	1	ReLU
Pooling layer-1		2 × 2	20 × 1 × 2045		2	
Convolution layer-2	8	9 × 1	20 × 8 × 2038	8 × 4 × 9/8	1	ReLU
Pooling layer-2		2 × 2	20 × 8 × 1019		2	
Convolution layer-3	16	9 × 1	20 × 16 × 1013	16 × 8 × 9/16	1	ReLU
Pooling layer-3		2 × 2	20 × 32 × 506		2	
Convolution layer-4	32	9 × 1	20 × 32 × 500	32 × 16 × 9/32	1	ReLU
Pooling layer-4		2 × 2	20 × 32 × 250		2	
Fully connected layer			100 × 1	100 × 8000/100		ReLU
Output layer			4 × 1	4 × 100/4		Softmax
Other parameters	Learning rate: 0.001; the maximum number of iterations: 320					

4.3. Analysis of Effect

The original signal of the input three different defects is decomposed by EMD, and the decomposition map of the 15 kV pollution pipe sleeve waveform is shown in Figure 15. According to the obtained IMF information, the network training is performed according to the set model parameters, and the obtained test results are shown in Figure 11. The overall defect recognition rate of the sample in the test set reached 95.3%. The recognition rates of insulation scratch, casing fouling, and joint loosening were 94%, 96%, and 94%, respectively. The ratios of wrongly considered joint loosening and insulation scratch were 9.4% and 4.1%, respectively. No defect was wrongly considered as casing fouling.

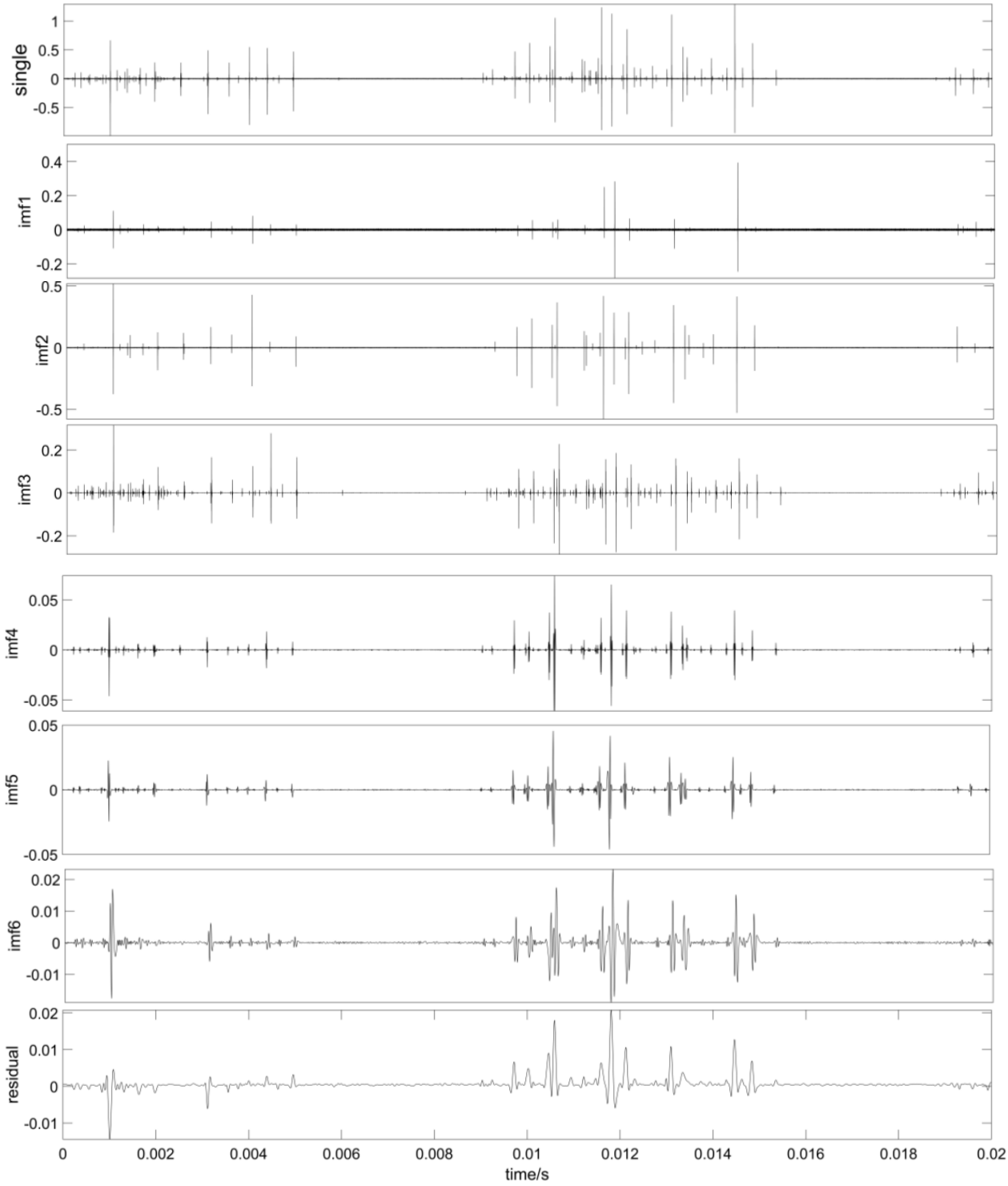

Figure 15. Charts of IMF components decomposed by EMD.

4.4. Comparison with Other Algorithms

In order to verify the effect of the model and algorithm, the random forest and EMD are compared with the DCNN algorithm, in which the former uses the random forest as the classifier. The Random Forest (RF) model is a supervised machine learning algorithm based on decision tree construction. The IMF information obtained after EMD decomposition is input into the RF model, and the recognition results are shown in Figures 16 and 17.

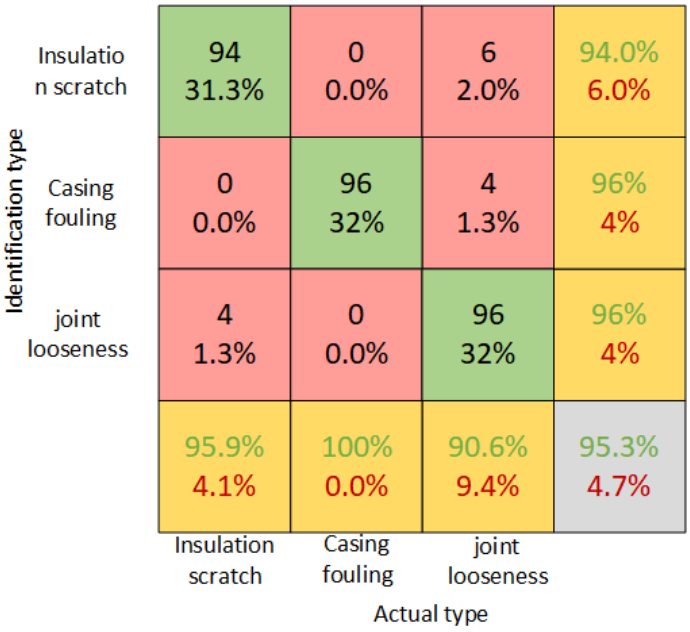

Figure 16. Recognition results of EMD and DCNN.

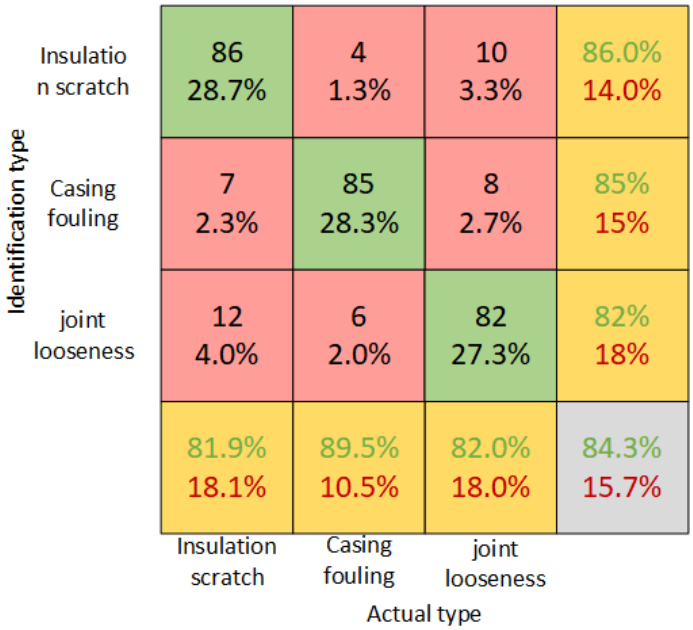

Figure 17. Recognition results of EMD-SVD-RF.

The identification of the two methods is shown in Table 5. It can be seen from Table 5 that the EMD–DCNN recognition method can better identify the three types of defects, and the average recognition rate is 95.3%. The average recognition rate of the traditional algorithm is only 89.7%. The EMD–DCNN recognition method is higher than the traditional mechanical learning algorithm, RF, in the recognition accuracy of each defect.

Table 5. Compares the results of the two algorithms.

Defect Type	EMD-SVD-RF Accuracy/%	EMD–DCNN Accuracy/%
Joint looseness	82	96
Casing fouling	85	96
Insulation scratch	86	94

SVD is a linear transformation that has a limited ability to express the characteristics of nonlinear signals. SVD can classify and recognize low-dimensional features. When dealing with high-dimensional data, training errors are easy to accumulate, resulting in distortion of training results, which cannot maintain the accuracy of recognition. In addition, SVD also needs to construct feature parameters manually, which has a great subjective influence. When the feature dimension is high, the training and inference time of RF is significantly increased, which makes the RF not ideal in scenes with high real-time requirements. In addition, the EMD–DCNN recognition method is also superior to the traditional mechanical learning algorithm, RF, in the recognition speed.

In this paper, EMD–DCNN is used as an improved CNN deep learning network model, which can directly process the image and retain the original information of the data structure. After multi-layer processing of the network and deep extraction of features, without human interference, the deep and shallow feature information of the data is automatically extracted layer by layer, and finally, a higher recognition rate and recognition speed are obtained.

5. Conclusions

This paper introduces the principle of empirical mode decomposition and the deep convolutional neural network model. The PD original signal of the T-type cable terminal is obtained by the experiment, and the IMF signal is obtained by EMD decomposition. The signal with characteristic information is used as input to identify the types of three kinds of T-type cable terminal defects obtained by the experiment. The recognition results of the proposed method and the traditional method are compared and analyzed. The conclusions are as follows:

(1) As an improved CNN network model, the EMD–DCNN network used in this paper can extract image features at a deeper level. Compared with the traditional model, it has a better recognition effect and faster training speed in partial discharge defect type recognition.
(2) In the process of sample training, the learning rate and the number of iterations have an impact on the recognition results of the improved CNN network. It has been verified that when the learning rate is 0.001 and the number of iterations is 320, the training recognition rate of the network can be stabilized at about 95%, and the network training loss value is also stabilized at a low level.
(3) The average recognition rate of the EMD and DCNN method proposed in this paper is 95.3%, while the average recognition rate of the EMD-SVD-RF method is only 89.7%, which is 5.6% lower than that of EMD–DCNN method, and the recognition rate of each defect is lower than that of EMD and DCNN method. In addition, the EMD–DCNN recognition method is also superior to the traditional mechanical learning algorithm, RF, in the recognition speed, which makes EMD–DCNN deal with real-time signals well.

Due to the above advantages, the EMD–DCNN method is more suitable for online monitoring platforms and applied to engineering practice. It reduces operation and maintenance costs at the economic level, extends equipment life, and promotes the development of intelligence and standardization at the technical level.

Author Contributions: Conceptualization, S.C.; methodology, S.C.; software, Y.G.; validation, C.F. and G.Z.; formal analysis, J.L.; investigation, S.C.; resources, C.F.; data curation, S.C.; writing—original draft preparation, S.C.; writing—review and editing, C.F.; visualization, J.L.; supervision, Y.G. All authors have read and agreed to the published version of the manuscript.

Funding: This research received no external funding.

Institutional Review Board Statement: Not applicable.

Informed Consent Statement: Not applicable.

Data Availability Statement: The data presented in this study are available on request from the corresponding author. The data are not publicly available due to privacy.

Conflicts of Interest: The authors declare no conflict of interest.

References

1. Li, S.; Li, J. Condition monitoring and diagnosis of power equipment: Review and prospective. *High Volt.* **2017**, *2*, 82–91. [CrossRef]
2. Khan, Q.; Refaat, S.S.; Abu-Rub, H.; Toliyat, H.A. Partial discharge detection and diagnosis in gas insulated switchgear: State of the art. *IEEE Elect. Insul. Mag.* **2019**, *35*, 16–33. [CrossRef]
3. Morette, N.; Ditchi, T.; Oussar, Y. Feature extraction and ageing state recognition using partial discharges in cables under HVDC. *Electr. Power Syst. Res.* **2020**, *178*, 106053.
4. Zhou, H.; Wan, D.; Zhao, M.; Fang, J.; Zhou, W.; Peng, S. Signal Recognition Method of Power Cable Oscillating Wave Partial Discharge Detection Based on Support Vector Machine. In Proceedings of the 2019 IEEE 3rd Conference on Energy Internet and Energy System Integration (EI2), Changsha, China, 8–10 November 2019; pp. 2334–2337.
5. Dong, Z.; Bao, F.; Hu, X.; Zeng, H.; Wu, Y.; Chen, Q. Cable Fault Identification Method Based on mRMR and Optimized Convolutional Neural Network. In Proceedings of the 2023 6th International Conference on Electronics and Electrical Engineering Technology (EEET), Nanjing, China, 1–3 December 2023; pp. 99–104.
6. Duan, L.; Hu, J.; Zhao, G.; Chen, K.; He, J.; Wang, S.X. Identification of partial discharge defects based on deep learning method. *IEEE Trans. Power Deliv.* **2019**, *34*, 1557–1568. [CrossRef]
7. Peng, X.; Li, J.; Wang, G.; Wu, Y.; Li, L.; Li, Z.; Bhatti, A.A.; Zhou, C.; Hepburn, D.M.; Reid, A.J.; et al. Random forest based optimal feature selection for partial discharge pattern recognition in HV cables. *IEEE Trans. Power Deliv.* **2019**, *34*, 1715–1724.
8. Peng, X.; Yang, F.; Wang, G.; Wu, Y.; Li, L.; Li, Z.; Bhatti, A.A.; Zhou, C.; Hepburn, D.M.; Reid, A.J.; et al. A convolutional neural network-based deep learning methodology for recognition of partial discharge patterns from high-voltage cables. *IEEE Trans. Power Deliv.* **2019**, *34*, 1460–1469. [CrossRef]
9. Zhang, G.; Quan, Y.; Qian, Z. Discharge signal Spectrum of Typical Office discharge Model of Power transformer. *High Volt. Technol.* **1999**, *2*, 13–14.
10. Hussein, R.; Shaban, K.B.; El-Hag, A.H. Robust Feature Extraction and Classification of Acoustic Partial Discharge Signals Corrupted with Noise. *IEEE Trans. Instrum. Meas.* **2017**, *66*, 405–413.
11. Raymond, W.J.K.; Illias, H.A. High Noise Tolerance Feature Extraction for Partial Discharge Classification in XLPE Cable Joints. *IEEE Trans. Dielectr. Electr. Insul.* **2017**, *24*, 66–74.
12. Huang, X.; Xiong, J.; Zhang, Y.; Liang, J. China Electric Power. In *Partial Discharge Pattern Recognition of Switchgear Based on Residual Convolutional Neural Network*; IOP Publishing Ltd.: Bristol, UK, 2020; pp. 44–51.
13. Mao, Z.; Li, F.; Ye, Y.; Wang, P.; Yuan, Q. Pattern recognition of cable partial discharge type based on BP neural network algorithm. *Mech. Electr. Inf.* **2019**, 20–22.
14. Mazzetti, C.; Mascioli, F.M.F.; Baldini, F.; Panella, M.; Risica, R.; Bartnikas, R. Partial discharge pattern recognition by neuro-fuzzy networks in heat-shrinkable joints and terminations of XLPE insulated distribution cables. *IEEE Trans. Power Deliv.* **2006**, *21*, 1035–1044. [CrossRef]
15. Wang, Y.; Fan, J.; Cai, H.; Zhao, K.; Wu, Y. Fault Diagnosis of Cylinder liner and piston Ring of Marine Diesel Engine based on improved Eemd-Mb1dcnn. *Mar. Eng.* **2019**, *53*, 30–35.
16. Aloysius, N.; Geetha, M. A Review on Deep Convolutional Neural Networks. In Proceedings of the 2017 International Conference on Communication and Signal Processing (ICCSP), Chennai, India, 6–8 April 2017; pp. 588–592.
17. Dhillon, A.; Verma, G.K. Convolutional neural network: A review of models methodologies and applications to object detection. *Prog. Artif. Intell.* **2020**, *9*, 85–112. [CrossRef]
18. Xie, S.; Girshick, R.; Dollár, P.; Tu, Z.; He, K. Aggregated Residual Transformations for Deep Neural Networks. In Proceedings of the 2017 IEEE Conference on Computer Vision and Pattern Recognition (CVPR), Honolulu, HI, USA, 21–26 July 2017; pp. 1492–1500.
19. Liu, Q.; Zhang, N.; Yang, W.; Wang, S.; Cui, Z.; Chen, X.; Chen, L. A Review of Image Recognition with Deep Convolutional Neural Network. In Proceedings of the International Conference Intelligence Computer, Odisha, India, 28 October 2017; pp. 69–80.
20. Ao, D.; Li, L.; Xu, Y. Image recognition and classification algorithm based on AlexNet. *J. Tianjin Vocat. Tech. Norm. Univ.* **2022**, *32*, 63–66.

21. Qun, S.; Qiukuan, Z.; Mingjun, L.; Zhiguo, T.; Da, Z. Recognition and Analysis of Transformer UHF Partial Discharge Signals based on Statistical Characteristics. *Electron. Devices* **2019**, *42*, 1394–1398.
22. Wang, J.; Fang, C.; Gao, G.; Cheng, H. Local discharge type identification of 10kV T-type terminal based on VMD-WVD and AlexNet. *J. Wuhan Univ.* **2024**, 1–9.
23. Jiaxin, L.; Yaoyao, Z. Improvement of EMD algorithm and its application in Signal denoising. *Electron. Manuf.* **2019**, *32*, 73–75.
24. Yuan, C. Mechanical Fault Diagnosis of vacuum Circuit breaker in Distribution Network based on EMD and neural Network. *China Mach.* **2024**, 96–98.
25. Li, X.; Shen, L.; Tian, Y.; Yin, J.; Wang, L.; Yang, D.; Mu, L.; Zhu, Y. Research on intelligent coal and rock identification method based on EMD and DCNN. *Coal Mine Mach.* **2024**, 45.
26. Zhao, Y. Application of deep learning in image recognition. *Inf. Comput.* **2019**, *36*, 126–128. [CrossRef]
27. Long, Y.; Jiang, C.; Zhong, Y.; Tian, Y. Transformer fault prediction based on deep learning network characteristics under extreme weather conditions. *Mod. Electron. Technol.* **2019**, *47*, 91–96.
28. Ru, J. Research on Transmission line fault prediction Method based on Deep learning. *Rural. Electrif.* **2024**, *2*, 1–5.
29. Jiang, J.; Chen, G.; Luo, Z. Research and Design of Rogowski Coil for Partial Discharge Signal Measurement. *High Volt. Appar.* **2025**, *61*, 63–71.